29th Congress of the International Council of the Aeronautical Sciences
St. Petersburg, Russia; September 7-12, 2014

ON THE FLIGHT OPERATING SAFETY IN THE MOUNTAINOUS ZONE AIRPORT

Konstantin Zudov *, Victor Vyshinsky *, Maxim Kudrov *
***Moscow Institute of Physics and Technology**

Keywords: *atmospheric turbulence, mountainous airport, numerical simulation*

Abstract

The statement of the terrain flow simulation problem is given in the paper, the computational mesh based on the contour map of the area is built, boundary conditions are stated.

The numerical simulation of the flow above the real mountain airfield Bakula Rimpoche (Leh, India) is performed. Wind direction that generates coherent vortex structures, crossing glide path and posing a danger to the aircraft performing takeoff and landing is found.

1 Introduction

Economic needs arouse the problem of secure schedule consolidation of the aviation traffic, construction and exploitation of the airports in the areas with adverse weather conditions, for instance, near an urban building or in conditions of mountainous terrain.

Unevenness of the heating of mountain slopes, located at different angles to the sunbeams and with different vegetation cover, may be the source of turbulence. Both condensation and evaporations zones, being the sources and sinks of energy are the sources of vorticity, as well. Consequences of falling into the powerful vortex structures during takeoff or landing can be disastrous due to the heavy loads acting on the aircraft and due to the trajectory perturbations, as well, which are mostly dangerous near the ground, especially in the case of the crew unavailability to perform correct actions.

A number of accidents can be explained by the aircraft falling into the areas with increased turbulence [1-3]. For example, on 3.05.2006 at 9:26 near Sochi, five kilometers from the coast, a disaster of A-320 «Armenian airlines», Flight 967 on the route Yerevan - Sochi, happened during the second landing. The aircraft steeply entered the water in the beam of Adler airport 5 kilometers from the coast.

With the growth of air traffic, the importance of the measures to ensure the safety in the airport area increases [1]. In particular, aviation faces a major problem - the lack of professionally trained pilots that can avoid emergency in complicated circumstances and in the case of it competently and quickly respond to the situation.

In confirmation, now we consider an accident of A300-600 aircraft that happened on 12.11.2001 (flight 587) in the United States. Shortly after takeoff from the Kennedy International Airport during the left turn (bank angle 23°) the aircraft crossed trailing vortex from B747-400 that had flown here not long before. Pilot unpreparedness to this situation (flight data recorder detected the increase in bank angle of only 2°) and «aggressive pilotage» (pedaling from lock to lock) caused yaw bobble and, as a result, vertical fin destruction.

Another urgent problem is the development of manned flight simulators for investigation of the problems related to atmospheric factors and aviation simulators for pilot training, that simulate the increased turbulence zone impact on the aircraft during takeoff, landing and missed approach in the area of a particular airport.

The feature of the problem is the large spatial and time scale: vortex can be potentially dangerous at long distances that imposes very

strict requirements on the research methods utilized.

Breezes, which behavior is especially complicated near the mountain terrain, can play a significant role for a seaside airport. In [8] the model of atmosphere boundary layer over the complex surface in the presence of breeze circulation is examined. Seaside location of the mountain airport complicates the problem due to the high air humidity. Flow around the mountain ridge in case of a rapid change of pressure and temperature results in vapor condensation. That causes visibility deterioration and increase in turbulence due to the release of energy. It was revealed in the flight conditions that water satiety in the prethunderstrom front could reach considerable magnitude [5]:

$$p_v / p_{vs} \approx 2,$$

where p_v – is vapor pressure, p_{vs} – is saturated-vapor pressure of the same temperature.

During some period atmosphere remains metastable. In case of a sudden condensation the heat of the phase transition is released. It is possible to upper estimate the temperature increment ΔT that goes along with this inner energy supply:

$$\Delta T = \frac{\rho_v L_{lv}}{C_p}.$$

Here ρ_v – is water vapor density, contained in the atmosphere; L_{lv} – is specific heat of phase transition; C_p – is air specific heat capacity. Assuming that ρ_v = 20 g/m^3, L_{lv} =2.5 MJ/kg, C_p = 1 kJ/kg·K, the temperature increment equals to $\Delta T \approx 50^{\circ}$C.

Naturally, such a significant heating may generate intense upward thermal that will substantially change the wind conditions around the airport. The sharp increase in temperature may result in the engine thrust reduction.

Dynamics of turbulent thermals with the regard to the phase transition was studied extensively. For example, in the monograph [6], the algorithms and the results of spatial vortex flows researches in nonhomogeneous atmosphere are presented.

Earth electrostatic field may have some influence on the wet wind flows gas thermodynamics in the mountain conditions. For instance, the field strength in normal conditions is in the order of 100 V/m, however this value may increase by two orders of magnitude under development of local voltages [4]. Strong electrostatic field polarizes the water microdroplets, what causes their interattraction and consolidation; this, in turn, may lead to visibility deterioration, or even to rainfall. Influence of the Earth electrostatic field and mountain terrain is studied in [8]. In addition, a large number of anthropogenic factors, affecting atmospheric and global processes is considered in [9].

A design of consistent, appropriate atmospheric model and vortex structures, admitting further development, refining and adjunction are placed in the focus of this problem.

Creating a system for wind vortex conditions monitoring in the area of the airport to help air traffic controllers may become possible in the nearest future.

2 Method of flowfield under mountain terrain numerical simulation

The boundary value problem for Reynolds Averaged Navier Stokes equations (RANS) is solved Shear Stress Transport (SST) closure model is used to simulate wind flows over the mountain terrain [17].

To solve the boundary-value problem for the RANS equations and SST turbulence model the following boundary and initial conditions are to be stated:

- Initial conditions for variables of RANS and SST models;
- Boundary conditions on the underlying terrain;
- Dirichlet conditions at the inlet of computational region ($(\vec{V},\vec{N}) > 0$, where $\vec{N}$ - is the outward normal to the boundary);
- Boundary conditions at the outlet of computational region $((\vec{V},\vec{N}) < 0)$ corresponding to non-reflective conditions.

No-slip, isothermality and the absence of turbulent fluctuations conditions are stated as

the boundary conditions on the underlying terrain.

At the inflow boundary the pressure is defined by Boltzmann distribution:

$$p = p_0 \exp\left[-Mg\frac{h-h_0}{RT}\right]$$

where p_0 - is pressure at zero level $(h-h_0)$, M - is air molar mass, R -is a molar gas constant, T - is an absolute temperature.

To state boundary conditions properly its necessary to have coordinated input profile of wind velocity and temperature, and with regard to their behavior in the ground sublayer and atmospheric boundary layer [18].

3 Velocity profile in the ground sublayer and atmosphere boundary layer

According to [18] under equilibrium conditions the mechanism of turbulent motion in the ground sublayer is similar to that which takes place in wind tunnels. Concerning air turbulent flows in a wind tunnel semi-empirical Prandtl theory of turbulence that describes properly the observed patterns is widely known in hydrodynamics. This theory can be directly applied to the ground sublayer under equilibrium conditions.

We now analyze the mixing length dependence. Obviously, near the underlying terrain mixing can not be large because the underlying terrain acts as a rigid wall bounding the movement of the turbulent eddies. Therefore, the mixing length should increase with the increase of height at least within a ground sublayer. Since both the mixing length and height are the dimensions of length, the simplest connection between them can be expressed by:

$$l = \chi z,$$

where χ — is a dimensionless constant, that should be universal. According to experiments $\chi = 0.38$. A study on the application of the hypothesis to the equilibrium conditions in the ground sublayer shown, that χ remains constant with the same magnitude here as well. Various authors have obtained χ value ranging from 0.36 to 0.43 which is apparently not beyond the influence of observational errors.

To study wind profile (i.e. vertical distribution) we now plug in the expression for friction induced shear stress τ the expression for l:

$$\tau = \rho\chi^2 z^2\left(\frac{\partial u}{\partial z}\right)^2.$$

After square rooting from the both sides of this equation and applying this notation for convenience:

$$v_* = \sqrt{\frac{\tau}{\rho}},$$

one may obtain the following relation:

$$v_* = \chi z\frac{\partial u}{\partial z}.$$

Variable v_* is called a dynamic velocity. It has velocity dimension, and uniquely associated with a specific stress of turbulent friction.

We now express and then integrate the velocity derivative from the formula for τ, and obtain the analytical form of the velocity profile:

$$u = \frac{v_*}{\chi}\ln z + C, \qquad (1)$$

where C — is a constant of integration.

Thus, under the equilibrium conditions, the wind profile in the ground atmosphere sublayer is logarithmic. If we denote by u_1 the wind velocity at a certain level z_1, such way that:

$$u_1 = \frac{v_*}{\chi}\ln z_1 + C.$$

Subtracting it from (1), we obtain the following relation:

$$u - u_1 = \frac{v_*}{\chi}\ln\frac{z}{z_1}. \qquad (2)$$

In the atmospheric physics, the patterns of turbulent motion both over the smooth and rough surfaces were studied. In a ground sublayer, smooth surfaces are almost never encountered as the underlying terrain always has some or other roughness. Therefore, we introduce the notion of roughness z_0.

The roughness can be obtained from the following considerations. We can assume that due to underlying terrain roughness the average velocity z_0 vanishes not on the underlying terrain but on some level above it, below which there are only turbulent perturbations.

Then, substituting in (12) $z_1 = z_0$, $u_1 = 0$, we obtain:

$$u = \frac{v_*}{\chi} \ln \frac{z}{z_0}.$$

According to the observations on the surface with artificial roughness of correct shape, value z_0 corresponds to about 1/30 of the height of the roughness. Wind profile measurements over vegetated land revealed that the surface roughness is about seventh or eighth of the height of vegetation.

According to [18], we use the following relation for the coefficient of eddy viscosity:

$$k = \chi v_* z. \qquad (3)$$

Equation (3) shows that the coefficient of eddy viscosity is significantly different in its properties from molecular coefficients, by analogy with which it was introduced. It is known that the coefficients of molecular viscosity, thermal conductivity and diffusion remains almost constant; they vary slightly only with the changes in temperature. In contrast, the coefficient of eddy viscosity varies significantly.

In fact, k strongly depends on the height, namely according to (3) it increases linearly with the increase of height under equilibrium conditions. But at a fixed altitude turbulence coefficient is not constant: as is clear from (3), it varies with the dynamic velocity v_*, i.e. proportionally to the square root of the friction stress. It can be conveniently written in the form:

$$k_1 = \chi v_*,$$

where k_1 — turbulence coefficient on the unit height z =1 m, therefore:

$$k = k(z) = k_1 z.$$

It is necessary to make the following observation. Usually wind velocity at levels of z more than 50 times higher than the roughness z_0 are of interest, so that formula (1) contains a larger value of the logarithm. However, the logarithm of the large value changes slightly with a small change of the argument. Consequently, when determining the wind, very approximate roughness parameters will be sufficient to know. Therefore, the definition of roughness is not often determined from gradient observations, but it can also be taken from the estimates [19]. In this paper, the parameter z_0 is set to be equal to 1 m.

Boundary layer of the atmosphere is the layer from the underlying terrain to the level of the order of 1-1.5 km, in which the vertical turbulent volume has a significant impact on the mean fields of meteorological elements [18]. The lower part of the atmospheric boundary layer is a ground sublayer that was considered earlier.

Plugging in the equation of horizontal motion [18], and taking into account the Coriolis acceleration:

$$\begin{cases} \dfrac{\partial u}{\partial t} - 2\omega_z v = -\dfrac{1}{\rho}\dfrac{\partial p}{\partial x} + N_x \\ \dfrac{\partial v}{\partial t} + 2\omega_z u = -\dfrac{1}{\rho}\dfrac{\partial p}{\partial y} + N_y \\ -g - \dfrac{1}{\rho}\dfrac{\partial p}{\partial z} = 0 \end{cases} \qquad (4)$$

the expressions for turbulent friction forces ($N_x = \frac{\partial}{\partial z}(k\frac{\partial u}{\partial z})$, $N_y = \frac{\partial}{\partial z}(k\frac{\partial v}{\partial z})$) [19] the following system of equations can be obtained:

$$\begin{cases} \dfrac{\partial u}{\partial t} = 2\omega_z v - \dfrac{1}{\rho}\dfrac{\partial p}{\partial x} + \dfrac{\partial}{\partial z}(k\dfrac{\partial u}{\partial z}), \\ \dfrac{\partial v}{\partial t} = -2\omega_z u - \dfrac{1}{\rho}\dfrac{\partial p}{\partial y} + \dfrac{\partial}{\partial z}(k\dfrac{\partial v}{\partial z}), \\ -g - \dfrac{1}{\rho}\dfrac{\partial p}{\partial z} = 0. \end{cases} \qquad (5)$$

It is worth noting that all terms of the right side of the resulting system of equations (5) describing the pressure gradient and turbulent viscosity are of the same order of magnitude. This suggests that in the hard core of the boundary layer, in contrast to the ground

sublayer, turbulent friction stress does not remain constant with the increase of height.

Currently, there are no well-founded theory about the nature of connection between turbulent interaction coefficient k in the boundary layer and the fields of main atmospheric physical quantities. There are only representations similar to semiempirical turbulence theory, applicable only in the ground sublayer. In the problem of the distribution of wind on height, we have to proceed from the certain hypotheses about the values of turbulent interaction coefficient and its reversing with altitude. The degree of credibilty of these hypotheses is tested by comparing the resulting conclusions about the wind distribution on height and the experimental data.

Factor k in the ground sublayer increases with the increase of height according to the law almost linearly. From the experiments, it can be concluded that this growth is slowing higher. Current data show that in the main body of the atmospheric boundary layer turbulent viscosity variation on height is small.

On the other hand, the correct value of k is not equally necessary in all the parts of the boundary layer. Since the effect of turbulent viscosity on the wind distribution decreases with the increase of height, then it is particularly important to know the value of the coefficient of eddy viscosity at the bottom, in the ground sublayer. At the top, the function $k(z)$ can be approximately described, just to avoid sharp differences with reality.

Currently, the most common pattern is a scheme with a break of the function $k(z)$, proposed by M.I. Yudin and M.E. Shwets [20]. Under this scheme, the coefficient of eddy viscosity is considered linearly increasing with the increase of height up to the upper boundary and constant down to the ground sublayer:

$$k = \begin{cases} k_1 z, & z < h; \\ k_1 h, & z \geq h. \end{cases} \qquad (6)$$

Based on this scheme, the model of wind distribution on height is built, which conforms to experimental data. We now consider this model with some simplifications. We assume that only the turbulent viscosity can be taken into account in the ground sublayer, i.e. that this layer has exactly the logarithmic wind profile derived from the linear profile of the turbulence coefficient. It can be shown that this assumption that simplifies calculations does not significantly affect the final results. However, it has some logical basis: linear growth coefficient of turbulent friction is closely connected with the constancy of stress and logarithmic wind profile.

Above the atmospheric boundary layer with a thickness of about 1 km wind direction is generally determined by the equilibrium of the pressure gradient and the Coriolis force. The resulting wind is called geostrophic. In the atmospheric boundary layer friction forces cause deviation of wind direction (in the northern hemisphere) to the left.

We now consider the motion without acceleration and assume at first that vector of horizontal pressure gradient does not depend on the altitude. If direct the x-axis along the isobar, the equations (15) can be written as:

$$\begin{cases} 0 = 2\omega_z v + \dfrac{\partial}{\partial z}\left(k \dfrac{\partial u}{\partial z}\right) \\ 0 = -2\omega_z u - \dfrac{1}{\rho}\dfrac{\partial p}{\partial y} + \dfrac{\partial}{\partial z}\left(k \dfrac{\partial v}{\partial z}\right) \end{cases} \qquad (7)$$

If introduce the geostrophic wind velocity $V_g = -\dfrac{1}{\omega_z \rho}\dfrac{\partial p}{\partial y}$ the system can be written as:

$$\begin{cases} 2\omega_z v + \dfrac{d}{dz}\left(k \dfrac{du}{dz}\right) = 0 \\ -2\omega_z u + \dfrac{d}{dz}\left(k \dfrac{dv}{dz}\right) = -2\omega_z V_g \end{cases} \qquad (8)$$

Here, instead of private the total derivatives are used as required functions u and v depend only on z.

According to the foregoing, the problem of a two-layer problem is necessary to solve. In the ground sublayer ($z \leq h$) all terms except of the first can be neglected, in the system of equations (8). In the ground layer, the shear stress is constant, therefore the wind direction will not change with the increase of height, and the velocity of the wind will be described by a logarithmic law with the hypothesis of a linear

dependence of the turbulence coefficient on the height:

$$V = \frac{k_1}{\chi^2}\ln(\frac{z}{z_0}),\ (z \le h)\ .$$

If we denote the angle α between the direction of the geostrophic wind and the wind in the ground sublayer, the velocity components in the ground sublayer can be obtained as:

$$\begin{cases} u = \frac{k_1}{\chi^2}\ln(\frac{z}{z_0})\cos(\alpha) \\ v = \frac{k_1}{\chi^2}\ln(\frac{z}{z_0})\sin(\alpha) \end{cases} \quad (z \le h) \quad (9)$$

In the main body of the atmosphere boundary layer $(z \ge h)$ the coefficient of the turbulent interaction is supposed to be constant and equal to $k_1 h,\ z \ge h$ so that system (8) in the upper region has the following form:

$$\begin{cases} k_1 h\frac{d^2u}{dz^2} + 2\omega_z v = 0 \\ k_1 h\frac{d^2v}{dz^2} - 2\omega_z u = -2\omega_z V_g \end{cases} \quad (z \ge h)\ (10)$$

The complex plane may be introduced, that is accepted by the reason of the equations linearity, not to solve the obtained equation system of the fourth degree:

$$W = u + iv\,. \quad (11)$$

By multiplying the first equation (10) by i and adding it to the second equation termwise the following equation may be obtained:

$$k_1 h\frac{d^2W}{dz^2} - 2\omega_z iW = -2\omega_z iV_g\,. \quad (12)$$

The global solution of this linear nonhomogeneous equation consists of the global solution of the W_0, corresponding to the homogeneous equation and any particular solution W_1 of the equation (12). As is easy to see the particular solution $W_1 = const = V_g$ exists.

The global solution of the equation:

$$k_1 h\frac{d^2W}{dz^2} - 2\omega_z iW = 0$$

is given by:

$$W_0 = C\exp(a\sqrt{2iz}) + D\exp(a\sqrt{-2iz})\,,$$

where C and D are some complex constants of integration; $a = \frac{\omega_z}{k_1 h}$ is the notation utilized for brevity.

Thus the wind profile in the is given by the following equation system:

in case $(z \le h)$:

$$\begin{cases} u = \frac{k_1}{\chi^2}\ln(\frac{z+z_0}{z_0})\cos(\alpha) \\ v = \frac{k_1}{\chi^2}\ln(\frac{z+z_0}{z_0})\sin(\alpha) \end{cases} \quad (z \le h)$$

in case $(z>h)$:

$$\begin{cases} u = V_g - \frac{k_1}{\chi^2}\sqrt{\frac{k_1}{2h\omega_z}}\,e^{-\sqrt{\frac{\omega_z}{k_1 h}}(z-h)}\cos\left[\sqrt{\frac{\omega_z}{k_1 h}}(z-h) + \frac{\pi}{4} - \alpha\right] \\ v = \frac{k_1}{\chi^2}\sqrt{\frac{k_1}{2h\omega_z}}\,e^{-\sqrt{\frac{\omega_z}{k_1 h}}(z-h)}\sin\left[\sqrt{\frac{\omega_z}{k_1 h}}(z-h) + \frac{\pi}{4} - \alpha\right] \end{cases}$$

Here h – is the distance to the surface in m (the thickness of the ground boundary).

The correction given hardly influences on the wind velocity in the common layer, it also eliminates the uncertainty.

The inlet coordinated temperature profile was created basing in the Monin - Obukhov theory [18] and was calculated by the method similar to the velocity profile.

In the ground layer according to the Monin-Obukhov model the coordinated linear-logarithmic profile is obtained:

$$\theta(z) - \theta(z_1) = -\frac{P_0}{\rho c_p \chi v_*}\left(\ln\frac{z}{z_0} - \beta\frac{z - z_0}{L}\right) \quad (13)$$

where $\theta(z)$ – is a potential temperature, P_0 – is a turbulent heat flow, L – is Monin-Obukhov scale, β=0.2.

Resulting inlet velocity and temperature profiles are shown in the Figures 1 and 2.

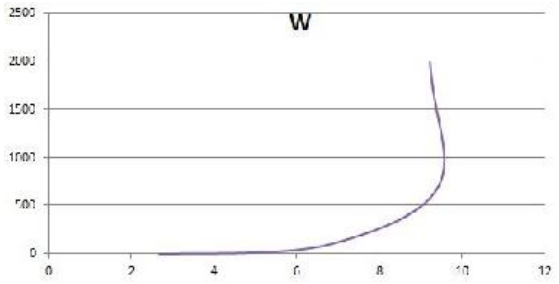

Fig. 1 – Resulting inlet velocity profile in m/s

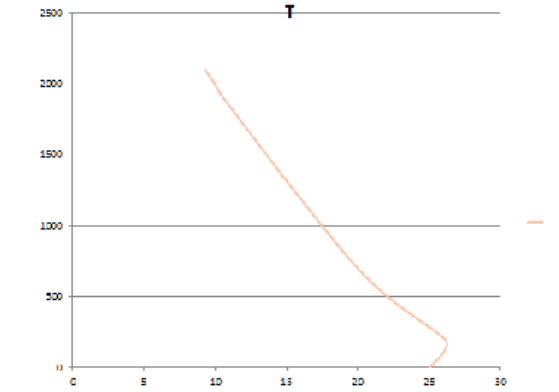

Fig. 2 – Resulting inlet temperature profile in degrees Celcius

The boundary conditions for the equations of the SST model are given in the following way. The turbulent kinetic energy is supposed to be equal to zero on the solid wall and its specific dissipation can be obtained from the formula:

$$\omega_w = 10\frac{6\nu}{\beta_1 \Delta y_1^{\,2}}$$

where ν – molecular kinematic viscosity, β_1 = 0.075, and Δy_1 – the height of the first near-wall mesh size.

On the inlet regions of the simulation domain outer boundary the value of the specific dissipation is set:

$$\omega_\infty = C\frac{U_\infty}{L}$$

where U_∞ and L – are the characteristic velocity and linear scales for this flow pattern, and the recommended values of the constant C vary in a range of 1-10. As for the value of the kinetic energy on the inlet boundaries, it is either stated directly (provided it is known from the experiment or derived basing on some physical assumtions) or calculated from the kinematic turbulent viscosity value on the inlet boundary $(\nu_t)_\infty$, which is assumed to be given: $k_\infty = \rho_\infty (\nu_t)_\infty \omega_\infty$.

4 The design of the underlying terrain

The digital model of the region terrain is built basing on the contour map plotted using the satellite observations data. This problem may be divided into two basic subproblems.

The first subproblem is to code and store contour map data, the second one is to decode the data stored and create the digital terrain model directly.

We now introduce some definitions connected to the terrain model creation.

When solving the problem mentioned the 3D mesh consisting of the organized sets of points and triangles was built. In this case every triangle (face) has three points (vertex) that are its vertices, as well. The sides of these triangles are called edges of the mesh. The common normal vector of the triangle is defined uniquely by the winding order and the thumb rule. Every point is located in the 3D space with the basic coordinate system given (X, Y, Z). By this means, the location of every triangle is defined in the space basing on the axes. Besides, the triangles store the data about their normal vectors. Different faces may either have the common vertices or not. In case two triangles have two common points then though their edges base on the same points they have different indexation. Due to this peculiarity the basic objects of the mesh are tringles. Besides, in general in this type of the mesh mentioned the data connected to the texture of the objects defined by mesh is stored.

Generally, Bitmap is the 2D organized set of pixels (dots of the image), though, there are no restrictions in the number of dimensions. Bitmap stores the data of the colour of the pixel in the colour channel with the accuracy required. There are many different storing extensions of the bitmap images, from which the TIFF extension (GeoTIFF) characterized with the colour depth reaching the value of 16 bit (65 535 variations) was chosen to be utilized in this problem. The heights coded with the use of the bitmap mentioned allow to store the data

with the accuracy till 1 m and the colour intensity corresponds to the height above the sea level.

To solve the problem stated the contour maps database ASTER (The Advanced Spaceborne Thermal Emission and Reflection Radiometer) GDEM (Global Digital Elevation Model) was used which is an open-source distributed by NASA (National Aeronautics and Space Administration), USA, and I (the Ministry of Economy, Trade, and Industry), Japan. All the data in this database provided by the USA are coded as the bitmaps in the GeoTIFF extension. In every file of such type the data about the altitudes in one squared degree, bounded by the parallels and meridians are stored. For instance, the nomenclature ASTGTM_N43E039 means that in this file the data about the heights in the area from 43° to 44° of northern latitude and from 39° to 40° of eastern longitude are stored. The resolution of the coded in bitmap data equals to the 3601 dimension per 1° along each axis (what equals approximately 30 m along the meridian).

For the purposes of further data stored in TIFF extension decoding process the Autodesk 3ds Max package software and its standard libraries 3ds Max and MaxScript were utilized, as well. With the use of this package, the opportunity to get the data about the absolute values of the heights in every point of space in the area required and create 3D mesh of the terrain based on the decoded data was obtained.

The algorithm of the mesh creation is as follows. The group of 4 points is chosen (2 neighborings from 2 neighboring rows) from the bitmap obtained by TIFF extension decoding. Basing on the values of these points 4 vertices are built of the virtual heights mesh in (X, Y, Z) space which corresponded to the real location of these points and the heights values coded via colour channel. Here, by the real location the cylindrical Earth projection in the 1:1 scale unfolded in a plane is meant.

Using 4 points of the space mentioned above, 2 faces were created, after what the procedure described above was repeated from the beginning. Thus by tracking all the bitmap points and building the triangles by the values corresponding to them all the mesh of the terrain heights in the vicinity of the mountainous airport used in further simulations was built. The algorithm of the creation of the model is depicted in the Figure 3 in a simplified form.

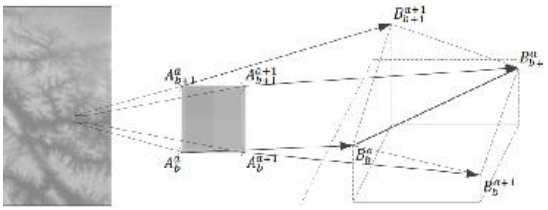

Fig. 3 – The scheme of the digital terrain model creation

The data obtained are stored then by means of the standard library MaxScript in the 3D mesh file of the .obj extension, which represents the full list of the triangle vertices coordinates, forming the terrain model stored.

The next step is to project the mesh of the terrain, obtained at the previous stage of the works, to 2 arcs with radii of 5786 and 4681 km respectively to provide the natural warp of the Earth surface.

Basing on the data obtained previously made from the initial bitmaps geometry file was created, where the points, surfaces and curves coordinates representing the terrain are stored. This file was obtained via exporting of the original mesh file with extension .obj to the extension .SAT with the use of temporary extension of 3ds Max mesh file .max. And the main parameter when choosing between two final mesh extensions was the high resource efficiency of the data importing process to the extension .SAT. The necessity of accomplishing such operations arouses by the peculiarities of the used in ANSYS 3D meshes, incompatible with the originally generated .obj file.

By the reason of the terrain having complicated topography and containing a large number of local maxima and angles, the creation of the multiblock structured computational mesh with a good quality seems to be impossible.

That is why the unstructed tetrahedral mesh with the structured prismatic sublayer on the terrain surface is built. Its creation is as complicated as the creation of the unstructed tetrahedral mesh, however it has near-wall block, analogous to the block of the structured

prismatic mesh. This block contains 25 nodes vertically with a total height of 100 m, the thickness of the near-wall node equals to 0.1 m and the ratio is 1.2 (the ratio of the vertical scales of two neighbouring nodes). In fact, the ratio of 1.2 is an optimal one: from one hand, it allows to avoid the appearance of non-physical gradients of the dependent variables, associated with the mesh nonuniformity, from the other hand, it doesn't lead to the extreamly large size of the mesh. The number of nodes in the block is 25 mln.

The outer domain of the mesh is a classic unstructed tetrahedral mesh. The volume of the outer mesh is ~35 mln of nodes. Their size increases with the increase of the distance to the terrain, what from the one hand allows to save computational resources and from the other hand it approximately doesn't influence on the quality of the solution obtained. The form of the underlying terrain, computational mesh above , on the boundaries of the computational domain and in one of the cross sections are shown in the Figures 4a-c.

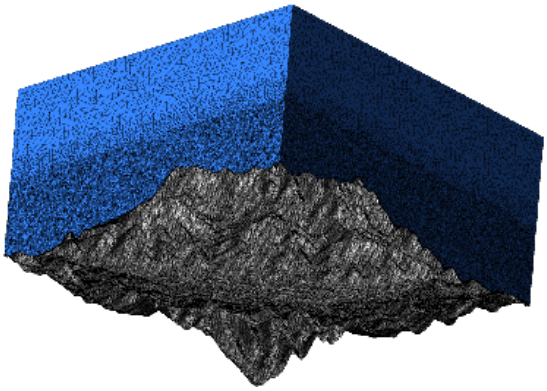

Fig. 4a– The terrain and form of the computational mesh on the side boundaries of the computational domain. The runway is approximately located in the middle of the terrain

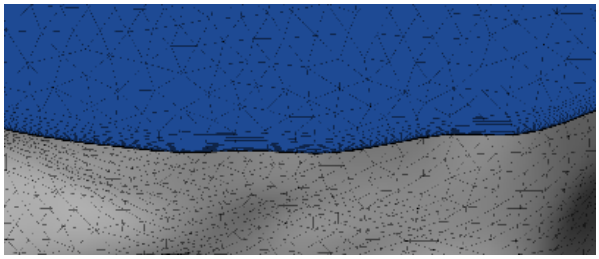

Fig. 4b – The form of the computational mesh on the underlying terrain and on the one of the boundaries of the computational domain

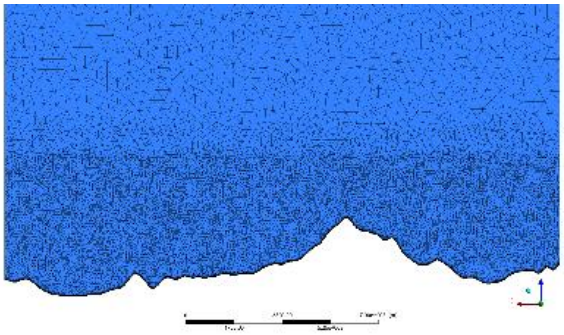

Fig. 4c – Cross section $z = 0$ of the computational domain (the form of the underlying terrain and computational mesh in this cross section)

5 The results of numerical simulation

The flow field above the terrain was obtained. Via numerical simulations on the diminished meshes the direction of the wind with which the vortex passing the airport location, ran off the mountains. The speed in the vortex core is 7.5 m/sec.

The visualization of the solution shows multiple vortex structure, their locations in the space, velocity and vorticity fields. In particular, the velocity increments are known in all the simulation domain of 20×20×10 km in size that allows to determine the increments of forces and torques acting on the aircraft vehicle flying with the determined angle of attack and velocity. One may also calculate the additional loads on the static aircraft, buildings and installations. The velocity field in the cross sections parallel to the runway in the Figure 5. The vorticity fields in different cross sections in the Figure 6. In the Figure 7 the speed distribution above the proposed location of the runway at the altitude of 400 m.

To visualize the vortex structures (Figure 8) the isosurfaces of lambda-2 were chosen [23]:

$$\left(\Omega_{ij}\Omega_{ij} - \mathbf{S}_{ij}\mathbf{S}_{ij}\right) = const\,,$$

where $\Omega_{ij}, \mathbf{S}_{ij}$ – vorticity and deformation tensors, respectively, which appears to be very convenient instrument in vortex visualization because it allows to cut nonuniformity of the boundary layer partly.

One may see in the given figures visualizing the vortex structures appearing due to the boundary layer separation their characteristic scale (>100 m) is sufficiently larger than the characteristic scale of the aircraft vehicles (~20 m), that is why the calculation of the increments of aerodynamic forces acting on the aircraft may be carried out in a simplified way. This means that we may carry out the numerical simulation of the homogeneous flow around the vehicle which covers it simultaneously in a range of different angles of attack, yaw and roll, corresponding to the oblique angle of velocity in the given point.

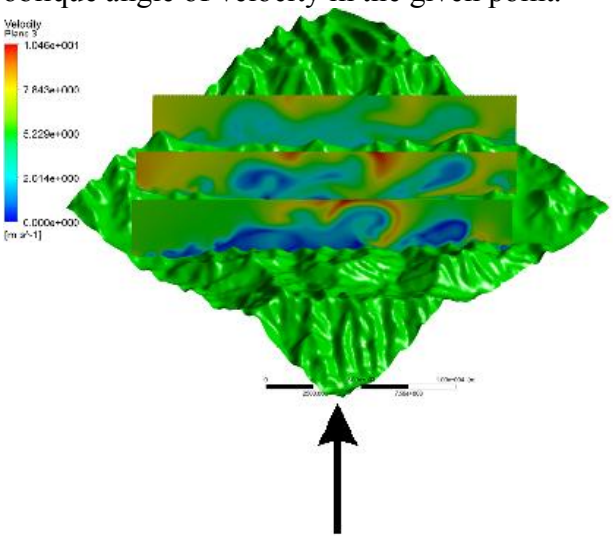

Fig. 5 – Speed field in different cross sections parallel to the runway direction. The wind direction is depicted by the arrow

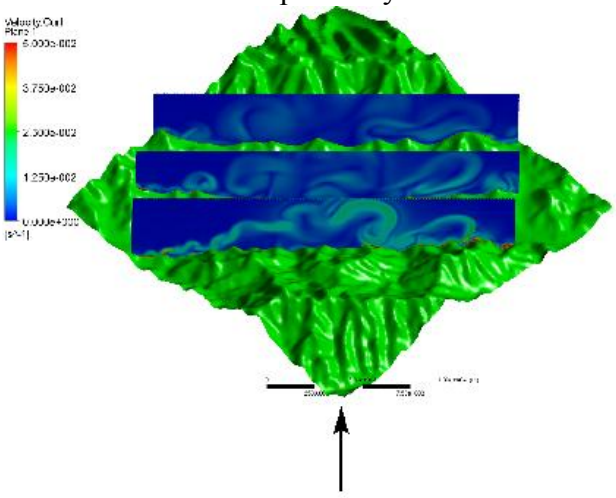

Fig. 6 – Vorticity fields in different cross sections, parallel to the runway direction. The wind direction is depicted by the arrow

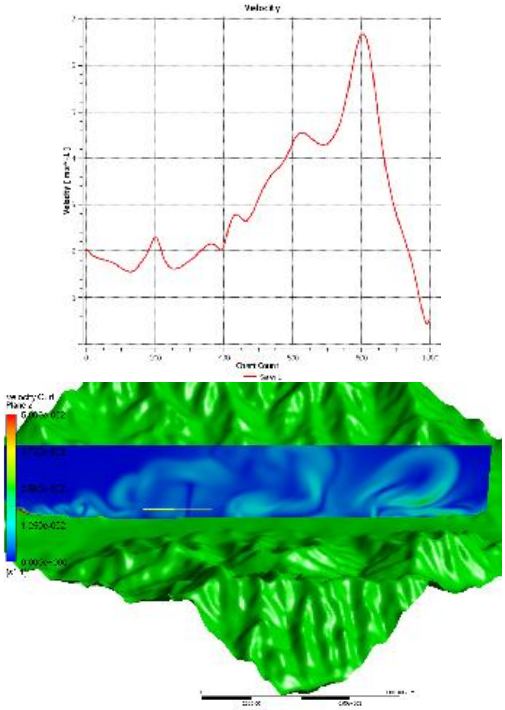

Fig. 7 – Speed distribution above the proposed runway location at the height of 400 m

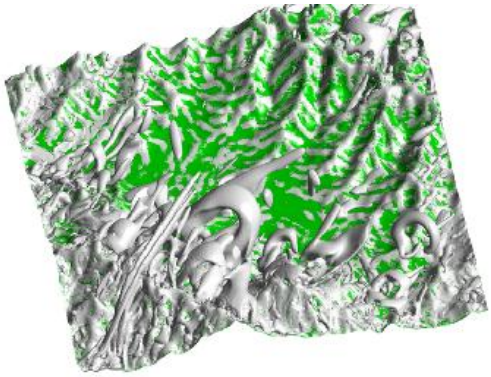

Fig. 8 – 3D vortex visualization with the use of lambda-2 function

This work is performed within the framework of the project “Development of the hardware/software complex of the pilot realistic perception of the complicated flight regimes and of the estimation of his psychophysiological status” (Contract No02.C25.31.0017).

References

[1] Vyshinsky V.V., Soudakov G.G. *Aircraft Trailing Vortex in the Turbulent Atmosphere (Physical and Mathematical Models)*. TsAGI, 2005.

[2] Vyshinsky V.V., Zamyatin A.N., Soudakov G.G. Theoretical and Experimental Research on the Trailing Vortex Evolution of the Aircraft in the

Atmosphere Boundary Layer. *Airfleet Engineering*. No. 3-4, pp. 25-38, 2006
[3] Vyshinsky V.V., Soudakov G.G. Aircraft Trailing Vortex and the Problems of the Flight Safety. *MIPT Proceedings*. Vol. 1., No 3. pp. 73-93, 2009.
[4] Ananyin I.V. Vortices in the Earth Crust and their Influence on the Surface Phenomena on the Earth. *XXX Academic Readings on Aeronautics Proceedings*. RAS Comission, 2006.
[5] Hilsenrath E. High Altitude Aircraft Water Vapor Measurements. *AIAA/AMS Intern. Conf. on the Environmental Impact of Aerospace Operations in the High Atmosphere*, Denver, Colorado, p 7, 1973.
[6] Bykov L.P. The Application of the Atmosphere Boundary Layer over the Complex Terrain for Studying the Circulation of the Breeze. *The Proceedings of the Main Geophysical Observatory*. No 454, pp. 97 – 108, 1981.
[7] Kudrov M.A., Stasenko A.L. The Dynamics of the Winged Aircraft Vehicle Aerosol Trailing Vortex over the Complex Terrain. *TsAGI Proceedings*. No 2676, pp. 52-59, 2008.
[8] Matveev L.T. *The Dynamics of Cloud*. Gidrometeoizdat, 1981.
[9] Dulov V.G., Belotserkovskiy V.M., Tsybarov V.A. *The Mathematical Simulation In the Global Problems of Nature*. SD RAS, 2005.
[10] Skorer R. *Aerodymanics of the Environment*. "Mir", 1980.
[11] Zhigulev V.N. *The Dynamics of Unstabilities*. MIPT, 1996.
[12] Frik P.G. *Turbulence: Models and Approaches*. Lectures. PSTU, 1999.
[13] Lapin Yu.V. Statistical Theory of Turbulence (Now and Then – a Brief Draft of Ideas). *Scientifically Technical Journal*, Feb. 2004.
[14] Toro E. *Riemann Solvers and Numerical Methods for Fluid Dynamic. A Practical Introduction*. Springer-Verlag Berlin Heidelberg, 2009.
[15] Spalart P.R., Jou W.H., Strelets M.K., Allmaras S.R. Comments on the Feasibility of LES for Wings and on a Hybrid RANS/LES Approach. *International conference on DES/LES*, Ruston, Louisiana, 1997.
[16] Menter F.R. Zonal two-equation k-omega Turbulence Models for Aerodynamic Flows. *AIAA Paper* 93-2906, 1993.
[17] Menter F.R., Kuntz M., Langtry R. Ten Years of Industrial Experience with the SST Turbulence Model. *Turbulence, Heat and Mass Transfer 4 / Ed. by K. Hanjalic, Y. Nagano, M. Tummers*. Begell House, Inc., 2003.
[18] Zilitinkevich S.S. *Atmosphere Boundary Layer Dynamics*. Hydrometeorological Publishment, 1970.
[19] Gandin L.S., Lightman D.L., Matveev L.T. *The Basics of the Dynamic Meteorology*. Hudrometeoizdat, 1970.
[20] *Hydrodynamic and Statistical Researches of the Atmospheric Processes*: *Collection of Articles*. *Editors M.I. Yudin, M.E. Shvets*. Hydrometeoizdat, 1976.
[21] J. Jeong and F. Hussain. On the Identification of a Vortex. *Journal of Fluid Mechanics*. 69-94. 285.

Contact Author Email Address

The contact author email address:

mailto:xzudov@mail.ru

Copyright Statement